4.3.2 Chemical shifts

The exact binding energy of an electron depends not only on the level from which photoemission is occurring, but also on the following:

1. The formal oxidation state of the atom
2. The local chemical and physical environment

Such shifts are readily observable and interpretable in XPS spectra (unlike in Auger spectra) because the technique (i) is of high intrinsic resolution (as core levels are discrete and generally of a well-defined energy) and (ii) is a one-electron process (thus simplifying the interpretation).

Atoms of a higher positive oxidation state exhibit a higher binding energy due to the extra coulombic interaction between the photoemitted electron and the ion core. This ability to discriminate between different oxidation states and chemical environments is one of the major strengths of the XPS technique.

4.3.3 Angle-dependent studies

The degree of surface sensitivity of an electron-based technique such as XPS may be varied by collecting photoelectrons emitted at different emission angles to the surface plane. This approach may be used to perform nondestructive analysis of the variation of surface composition with depth (with chemical state specificity).

4.3.4 Experimental details

The basic requirements for a photoemission experiment (XPS or UPS) are as follows:

1. A source of fixed-energy radiation [an x-ray source for XPS or, typically, an He discharge lamp for ultraviolet photoelectron spectroscopy (UPS)]
2. An electron energy analyzer (which can disperse the emitted electrons according to their kinetic energy and thereby measure the flux of emitted electrons of a particular energy)
3. A high-vacuum environment (to enable the emitted photoelectrons to be analyzed without interference from gas phase collisions)

If studies of photo- and thermodegradation of the organic active layer, which can play an important role in the loss of the optoelectronic properties of the devices, are crucial in order to improve organic solar cells stability,[17–19] another essential point to understand is the chemical and morphological evolution during aging of the electrodes and principally at the electrode-organic active layer interfaces. It has previously been shown that the initial degradation of OPVs strongly depends on the material used as the cathode.[20] In most of the studied organic solar cells, a thin lithium fluoride (LiF) layer adjunction between metal cathode (generally aluminum) and organic active layer has demonstrated an overall improvement of electrical characteristics.[21] It is well known that insertion of a thin barrier layer prevents interaction between the deposited cathode and active layer. It may be an

explanation of the improvement of the devices compared to an Al-only cathode, for example, but is not an exhaustive explanation. During the past 10 years of development for OLEDs, the insertion of a LiF layer between a stable metal such as Al and the organic emitting layer has provided better efficiencies, particularly with a decrease in the operating voltage.[22–24] Using UV photoelectron spectroscopy, this improvement was ascribed to an enhanced electron injection at the cathode by a reduction of the barrier height between the LUMO of the organic layer and the work function ($\Phi_{\mathrm{electrode}}$) of the aluminum cathode and band bending phenomena in the LiF layer.[25,26] This reduction improves as the built-in potential ($V_{\mathrm{BI}} = \Phi_{\mathrm{anode}} - \Phi_{\mathrm{cathode}}$) of the device and can be directly related to the decrease of Φ_{cathode}. The variation of the work function for aluminum is found to be dependent on the thickness of LiF.[27]

Two explanations can be found in the literature that describe how Φ_{cathode} decreases, as follows:

1. Dissociation of alkali fluoride. This is still controversial but observed in the case of small molecules such as tris(8-hydroxyquinolinato)aluminum (Alq3) and for polymers such as MEH-PPV, giving rise of a low work function contact and/or doping phenomena in the organic layer with free Li.[28,29]
2. Generation of a dipole in LiF layer that induces a shift between the vacuum levels of the cathode and organic compound that thus lowers the Φ_{cathode}.[26]

Because of the hygroscopic nature of LiF, deposition conditions seem to be important in interfacial mechanisms that occur. On one hand, H_2O molecules promote reaction between aluminum and LiF,[30] and on the other hand, chemisorption of a few monolayers of H_2O would result in a strong interface dipole between aluminum and LiF.[26]

Experimentally, the LiF layer does not behave as a good insulator[31] and has a nonuniform coverage at low thickness[32] that can diminish the voltage drop at the interface. Studies at Linköping University regarding interfaces between Al, Li, or Al/Li cathodes and PFO [poly(9,9-dioctyl-fluorene)],[33] and studies by Gennip and coworkers with poly(p-phenylene vinylene) and PCBM,[34] are particularly interesting. In the case of PFO, neither appearance of new gap states nor dissociation of LiF takes place for Al/LiF/PFO devices. No indication of interaction at the interface Al/LiF/MDMO (or PCBM) is observed. Formation of AlF_3 as well as Li doping was eliminated as a possibility by SIMS studies. Evidence of the formation of a surface dipole at the LiF/Al interface and the observation that the LiF layer protects PFO and PCBM from interaction with Al (no interaction between MDMO-PPV and aluminum is observed) has been found. A thin layer of LiF does not seem to interact with the cathode or the organic layer.

In this section, we describe results obtained by XPS studies of the cathode–active layer interface for a typical Al/LiF/MDMO-PPV:PCBM/PEDOT:PSS/ITO/glass solar cell in its freshly prepared form and after aging (for tens of hours) under illumination in an oxidative atmosphere. Several possible physicochemical changes

were revealed concerning the (not well-defined) action of the LiF layer that could be responsible for the rapid degradation of the unencapsulated devices.

To study the chemical and morphological changes taking place at the cathode–active layer interface, we have decided to look into three types of samples. To demonstrate alterations that occurred at the interface under aging, we have compared a complete solar cell kept in the dark in ambient atmosphere (labeled "not-aged cell"). One cell was aged during some tens of hours under illumination in an oxidative atmosphere (labeled "aged cell"). Keeping in mind that we use ionic sputtering to probe the interface in this device, we have also directly characterized reference devices without cathode, with a 1 nm LiF cathode, and 2–10 nm Al on 1 nm of LiF. By comparison of the reference devices with the not-aged solar cell, we were able to distinguish "real" aging effects from the effects created during etching using argon ion sputtering. Argon ion implantation and collision with the constituents of the the exposed volume of the cathode could lead to movement and rearrangement of the target components.[35]

4.3.5 Device aging and IV measurement

The aging chamber was under a controlled oxidative atmosphere. During aging, the current-voltage characteristics were recorded with a Keithley SMU 2400 unit. The devices were illuminated with a halogen photooptic lamp (Xenophot®) with a light intensity at the sample position of 63 mW cm^{-2} illumination. The temperature in the aging chamber was measured using a thermocouple (Pt100) and was found to be constant around 30°C during aging. Before introduction of the oxidative atmosphere in the test chamber, the IV characteristics of the cell were recorded (Fig. 4.29). After the first hours of aging, we observe a quick decrease of the open-circuit voltage (V_{oc}) from 0.75 to 0.7 V and a decrease in the fill factor (FF) from 0.52 to 0.45. The decrease of the FF is mainly linked to the increase of the

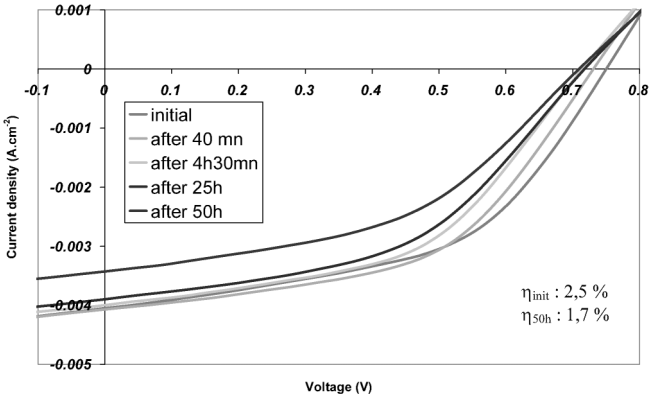

Figure 4.29 Evolution of IV characteristic during aging of an Al(50 nm)/LiF(1 nm)/MDMO-PPV:PCBM(70 nm)/PEDOT:PSS/ITO/glass solar cell.

series resistance R_s of the cell. The shunt resistance (R_{sh}) stays almost constant even after 50 hr of working.[36–38] The short-circuit current density starts to decrease significantly after 10 hr of illumination. After 50 hr of aging under the experimental conditions, the power conversion efficiency drops to about 30%.

The evolution of the IV characteristics of the solar cells during the first hours of operation is similar to the IV characteristics of ITO/PEDOT/MDMO-PPV:PCBM/Al with or without insertion of an LiF layer.[32,40] These macroscopic observations strengthen the idea that chemical and/or morphological changes occur around the Al/LiF–active layer interface and that the proposed beneficial properties of the LiF layer can be questioned.

4.3.6 XPS overall observations

Characterization of the interface between the active layer and the cathode was performed in an ultrahigh vacuum setup where manipulation of the sample between two chambers is possible at a pressure of around 7×10^{-9} mbar as follows:

1. The first chamber is an etching station comprising an AG21 Argon ion gun (VG Microtech). One of the manipulation difficulties was to probe the interface buried under the cathode. Sputtering with Ar ions allows for etching through the aluminum cathode. To avoid too many target degradations during ion etching, a low energy was applied. However, SRIM03 simulation, using Monte Carlo calculations to make detailed calculations of the energy transferred to every target atom by collision, revealed that correct energies for sputtering/etching, that is, sputtering yield = (number of sputtered atoms)/(number of incident ions) larger than 4, were above 2 keV. In the experiments reported here, an energy of 3 keV was used for Ar ion sputtering with currents of a few microamperes. Experiments with 2 keV Ar ions showed identical results in depth profiles.
2. The second chamber has the XPS source and analyzer. Photoemission studies were performed with a Vacuum Generator Escalab 210 spectrometer, using the monochromatized Al-Kα line at 1486.6 eV. A fixed analyzer pass energy of 20 eV was used for element core level scans and 50 eV for survey scans. The photoelectron takeoff angle was 90 deg with respect to the sample plane, which provides an integrated sampling depth of approximately 10 nm. The energy scale of the instrument was calibrated by setting Au $4f_{7/2} = 84.00$ eV [with full width at half maximum (FWHM) at 0.95 eV], $Ag3d_{5/2} = 368.70$ eV.[39] The core level signals from the elements were decomposed using mixed symmetrical Gaussian-Lorentzian curves. For all the analysis, the Gaussian character varied between 50% and 90% and the FWHM between 0.8 and 1.8 eV, except for the mentioned elements. No energy compensation was applied. The fitting procedure used the standard Vacuum Generator instrument software, which solves the matrix of derivatives of the peak parameters with a Gaussian-Newtonian method to locate a minimum in the residual-root-mean square between the experimental

data and the fitting curve. The best fit obtained by varying the number of peaks and their location on the energy scale was retained.

Going back and forth between sputtering station and XPS, we were able to trace a depth profile of the different elements found in the device. Depth profiles of the aged and nonaged diodes permitted us to follow elements detected from the surface of the aluminum cathode to the active layer (Fig. 4.30). First, in Fig. 4.30(a), we observe mainly Al and O in the Al volume. Then, when the metal-organic interface is reached (Fig. 4.30(b)], Al peaks start to decrease and F, Li, and C increase until the organic layer. When Al, F, and Li disappear, only C, O, and S elements can be easily seen (Fig. 4.30). The presence of sulfur is attributed to the MDMO-PPV precursor. The presence of argon is due to its implantation during etching; its content is relatively low ($<$4 atom%).

The first aging effect is the detection of indium and tin in an oxidized form at the interface of the aged device [Fig. 4.30(b)]. These two elements are not observed in the case of not-aged solar cells. The ratio In:Sn found is around 10:1. These peaks are still present but at lower amounts in the active layer [Fig. 4.30(c)]. A part of the ITO anode compounds [In_2O_3 or $In(OH)_3$, and SnO_2 or $Sn(OH)_4$ species with binding energy 445eV for $In(3d_{5/2})$ and 486.7eV for $Sn(3d_{5/2})$][42–45] diffuse across both organic layers (PEDOT:PPS and MDMO-PPV:PCBM) as far as the cathode-organic interface when the cell is operating under illumination. This result gives an extension of the formation of an interfacial layer with indium and tin from the ITO that has diffused through the active layer. This effect has been observed in aged diodes.[46]

In Fig. 4.31, the quantitative evolution of O compared with Al and C gives information about oxygen distribution and its diffusion during aging of the cells. First, in the case of the nonaged cell, there is some native oxidation of aluminum at the surface of the cathode and a notable amount of oxygen at the metal-organic interface is also present. After aging, a presence of oxygen in the bulk of the Al cathode is observed and this is ascribed to the porosity of the Al cathode. Furthermore, the oxygen content increases at the metal-organic interface. Oxygen accumulation at the metal-organic interface has already been reported in a TOF-SIMS study of the Al/C_{60} interface of a Al/C_{60}/C_{12}-PPV/PEDOT:PSS/ITO/glass device under illumination in the presence of an isotopically labeled oxidative atmosphere.[12]

4.3.7 Li and F distribution

To properly compare Li and F in XPS studies, it is important to take the mean free path (mfp) of emitted photoelectrons into account because of the great difference of the binding energy of these elements [around 56 eV for mean peak Li(1s), and 686 eV for F(1s)]. According to Penn's calculations,[47] mfp(Li) is around 50% greater than mfp(F). In the case of a homogenous distribution of Li and F, elements in the LiF layer Li should be observed first when probing the cathode–active layer interface. Another important point is that the XPS detection of lithium is more

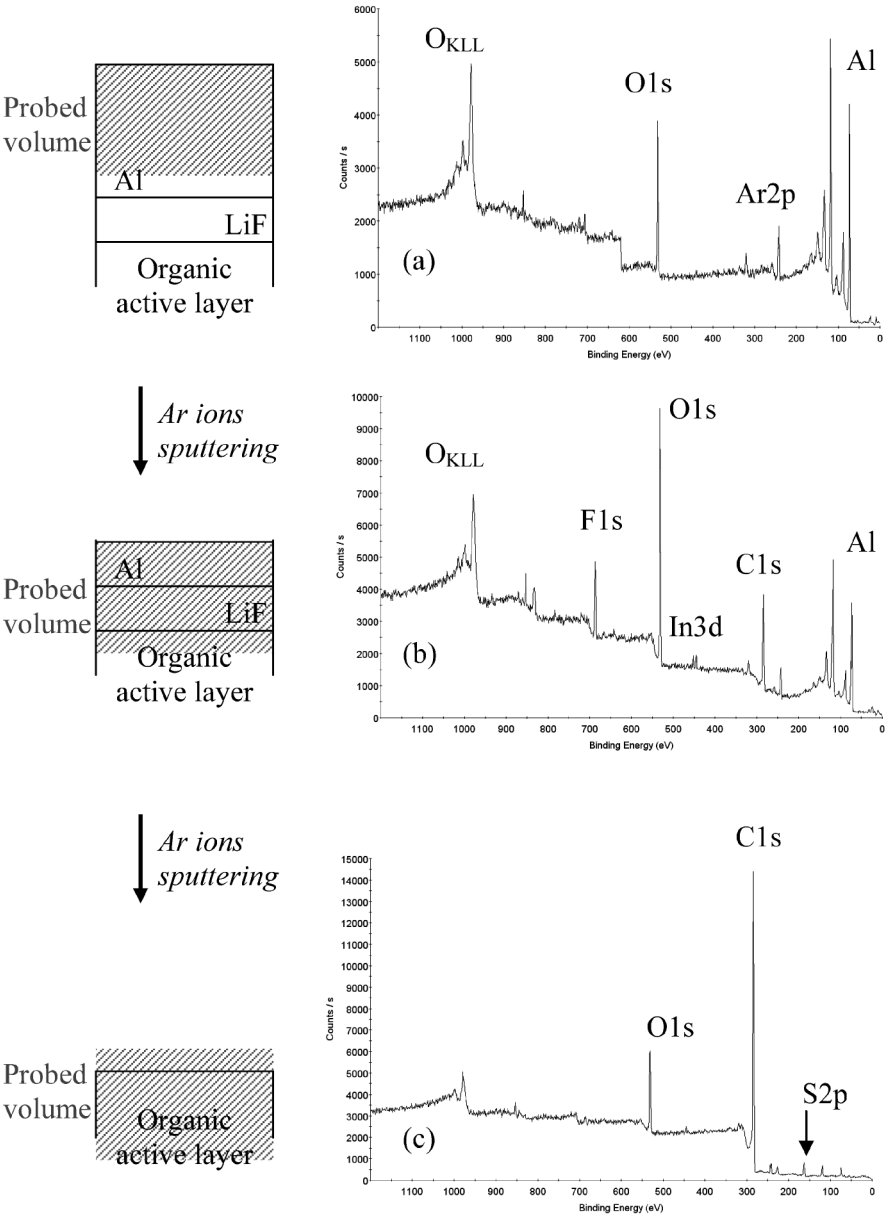

Figure 4.30 Evolution of XPS survey scans after cathode sputtering into aged cells: (a) Al cathode, (b) at the Al/LiF/active layer interface, (c) organic active layer (only the greatest peaks are noted).

difficult than fluorine because of the smaller cross section of Li atoms than F atoms. To compensate for this point, a great number of scans have to be accumulated for Li atoms (typically a few hundred scans) compared to F atoms (tens of scans).

Quantitative depth profiles of Li and F elements are shown in Fig. 4.32. Before and especially after illumination of the solar cell, different depth profiles for F

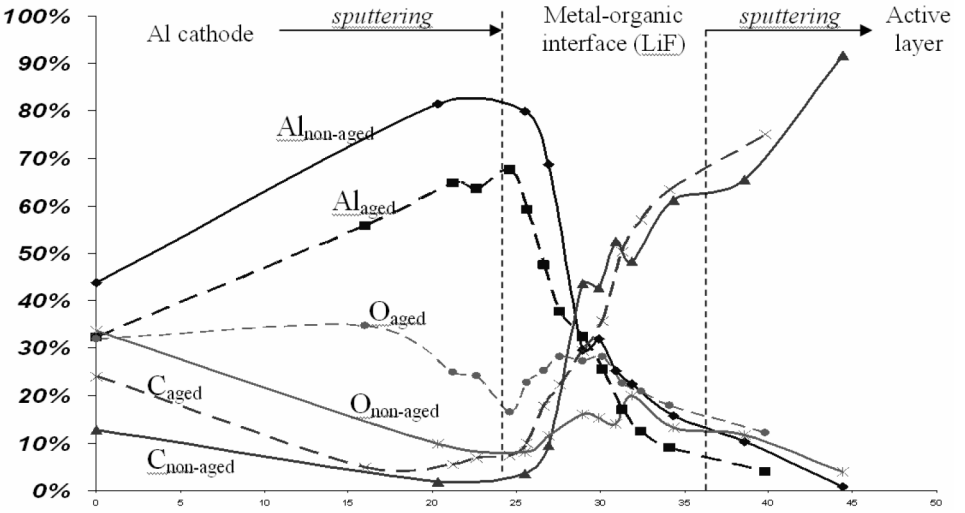

Figure 4.31 Percent atomic depth profile of main elements Al, C, and O read. Nonaged cell in solid line, and aged cell in dashed line.

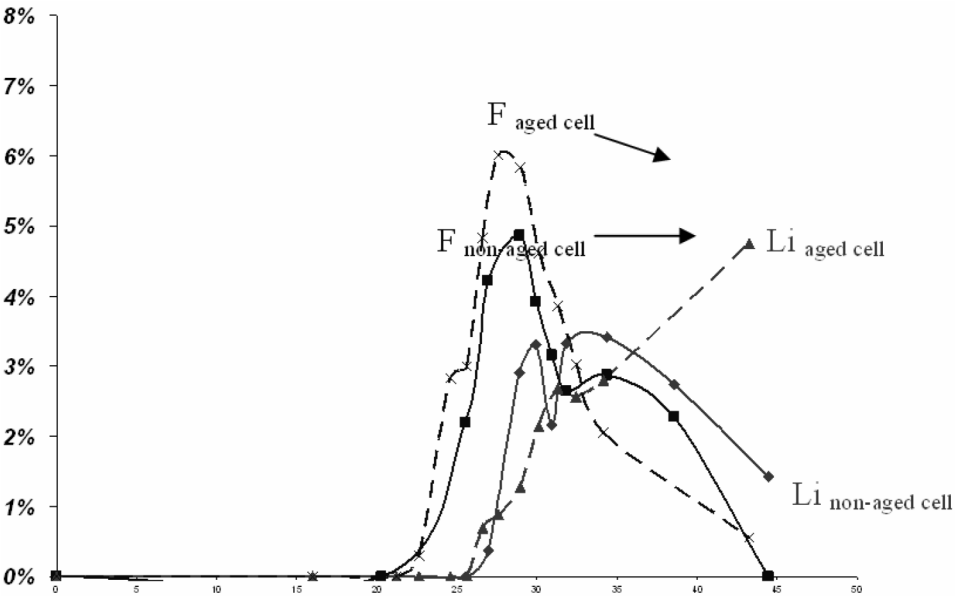

Figure 4.32 Percent atomic depth profile of main elements Al, C and O read. Non-aged cell in full line and aged cell in dashed line.

atoms are observed when compared to the depth profiles of Li atoms. Fluorine seems to be concentrated near the Al/LiF interface, whereas lithium is concentrated near the LiF–active layer interface. Thus, the distributions of Li and F elements are not homogeneous, as discussed above.

For aged devices, the fluorine distribution does not seem to vary with depth, while the lithium distribution seems to diffuse toward the polymer layer. To determine if this diffusion phenomenon is only due to the sputtering process or if it is a redistribution or reorganization of the interface, we have considered two cases.

SRIM03 simulation of the Al/LiF/polymer multilayer structure under ionic sputtering does not show any prevalence of transfer of Li or F atoms (Fig. 4.33). The simulation informs us about the overall distribution of Li, and F as obtained experimentally (especially around the interfaces). SRIM03 does not take chemical effects of Ar sputtering process into account and gives only a clue about the origin of the different depth distributions of Li and F atoms.

We have observed lithium and fluorine depth profiles in nontreated Al(4 nm)/LiF(1 nm)/MDMO:PPV systems by variation of the angle between XPS detector and the normal of the sample (Fig. 4.34). The greater angle that is used, the nearer surface of the device is probed. In order to try to understand the observed quantitative profile, we have to take into account both photoelectron mean-free-path and heterogeneous distribution of Li and F at the interfaces.

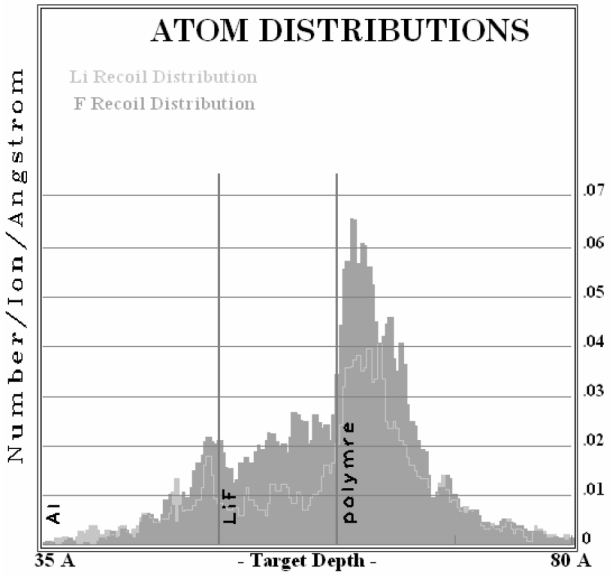

Figure 4.33 SRIM03 simulation of recoiled Li and F atoms distributions in [Al (5 nm)/LiF (1 nm)/polymer (70 nm)] system after Ar^+ (3 keV) sputtering (after 5000 counts). Densities applied were 2.702 for Al, 0.8225 for LiF, and 2.3 for polymer.